


RESEARCH

Open Access



A genome-wide RNA interference screening reveals protectiveness of *SNX5* knockdown in a Parkinson's disease cell model

Matthias Höllerhage^{1,2†} , Linghan Duan^{1†}, Oscar Wing Ho Chua¹, Claudia Moebius³, Svenja H. Bothe¹, Kristina Losse¹, Rebecca Kotzur⁴, Kristina Lau^{2,4}, Franziska Hopfner⁵, Franziska Richter^{2,4}, Christian Wahl-Schott⁶, Marc Bickle³ and Günter U. Höglinger^{5,7,8*}

Abstract

Background Alpha-synuclein (αSyn) is a major player in the pathophysiology of synucleinopathies, which include Parkinson's disease, dementia with Lewy bodies, and multiple system atrophy. To date, there is no disease-modifying therapy available for these synucleinopathies. Furthermore, the intracellular mechanisms by which αSyn confers toxicity are not yet fully understood. Therefore, it is of utmost importance to investigate the pathophysiology of αSyn-induced toxicity in order to identify novel molecular targets for the development of disease-modifying therapies.

Methods We performed the first genome-wide siRNA modifier screening in a human postmitotic neuronal cell model using αSyn-induced toxicity as a read-out. In a multi-step approach, we identified several genes, whose knockdown protected against αSyn-induced toxicity. The main hit was further validated by different methods, including immunofluorescence microscopy, qPCR, and Western blot. Furthermore, the main finding was confirmed in mouse primary neurons.

Results The highest protection was achieved by knockdown of *SNX5*, which encodes the sorting nexin 5 (SNX5) protein, a component of the retromer complex. The protective efficacy of *SNX5* knockdown was confirmed with an independent siRNA system. The protective effect of *SNX5* knockdown was further confirmed in primary neurons from transgenic mice, where the knockdown of *SNX5* led to amelioration of decrease in synchrony that was observed in untreated and control-siRNA-treated cells. SNX5 protein is a component of the SNX-BAR (Bin/Amphiphysin/Rvs) heterodimer, which is part of the retromer complex. Extracellular αSyn and overexpression of intracellular αSyn led to fragmentation of the trans-Golgi network, which was prevented by *SNX5* knockdown that led to confinement of αSyn in early endosomes.

Conclusion In summary, our data suggest that SNX5 plays an important role in the trafficking and toxicity of αSyn. Therefore, SNX5 appears to be a target of therapeutic intervention for synucleinopathies.

Keywords Genome-wide RNAi screening, Parkinson's disease, Alpha-synuclein, Retromer, SNX5, Trans-Golgi network

[†]Matthias Höllerhage and Linghan Duan have contributed equally to this work.

*Correspondence:
Günter U. Höglinger
Guentar.Hoeglinger@med.uni-muenchen.de
Full list of author information is available at the end of the article



© The Author(s) 2025. **Open Access** This article is licensed under a Creative Commons Attribution 4.0 International License, which permits use, sharing, adaptation, distribution and reproduction in any medium or format, as long as you give appropriate credit to the original author(s) and the source, provide a link to the Creative Commons licence, and indicate if changes were made. The images or other third party material in this article are included in the article's Creative Commons licence, unless indicated otherwise in a credit line to the material. If material is not included in the article's Creative Commons licence and your intended use is not permitted by statutory regulation or exceeds the permitted use, you will need to obtain permission directly from the copyright holder. To view a copy of this licence, visit <http://creativecommons.org/licenses/by/4.0/>. The Creative Commons Public Domain Dedication waiver (<http://creativecommons.org/publicdomain/zero/1.0/>) applies to the data made available in this article, unless otherwise stated in a credit line to the data.

Background

Synucleinopathies are a group of neurodegenerative diseases defined by the presence of intracellular proteinaceous inclusions consisting mainly of aggregated alpha-synuclein (α Syn). In cases of PD and dementia with Lewy bodies, these α Syn aggregates are found in neurons and designated as Lewy bodies [1]. Multiple system atrophy is characterized by α Syn aggregates, called glial cytoplasmic inclusions, in oligodendrocytes [2]. Physiologically, α Syn is a small, unfolded and soluble protein of 140 amino acids. However, in synucleinopathies, α Syn aggregates and confers neuronal toxicity. In PD, the typical motor symptoms (bradykinesia, rigidity, and tremor) are caused by the death of dopaminergic neurons in the substantia nigra pars compacta. It is widely accepted that α Syn plays a role in synapses [3]. The mechanisms of how α Syn becomes toxic are not fully understood. However, a common assumption suggests that small oligomeric species occurring in the aggregation process are toxic for neuronal cells [3]. Furthermore, the release of α Syn into the extracellular space and the uptake of α Syn species by neighboring cells are believed to play a role in cell-to-cell spreading of α Syn pathology throughout the brain, which is considered a mechanism involved in the progression of the disease [4]. In order to investigate α Syn pathophysiology, we established a model in differentiated, postmitotic dopaminergic Lund human mesencephalic (LUHMES) neurons [5], in which moderate overexpression of human wild-type α Syn leads to ~50% of cell death, accompanied by the occurrence of a 37-kDa oligomeric species of α Syn that was not present in control cells [6]. In this model, we have previously investigated intracellular mechanisms involved in α Syn degradation and identified protective interventions [7–9]. In the present work, we performed a genome-wide siRNA screening in this model to identify genes whose knockdown protects against α Syn-induced toxicity. The most interesting hit was sorting nexin 5 (SNX5), a member of the retromer complex, which is a cargo recognition complex involved in endosome sorting and endosome–trans Golgi network (TGN) trafficking [10].

Since mutations in vacuolar protein sorting ortholog 35 (VPS35), another component of the retromer complex, are associated with hereditary forms of PD [11], and endocytosis and endosomal trafficking have been linked to uptake and release of α Syn [12], our focus was to investigate the involvement of SNX5 in the regulation and trafficking of α Syn and how SNX5 gene knockdown protects dopaminergic neurons from α Syn-induced cytotoxicity.

The aim of this study was to perform a genome-wide siRNA screening in order to identify novel molecular targets for a potentially disease-modifying therapy

for neurodegenerative synucleinopathies, and perform a deeper characterization of the main hit from this screening.

Methods

LUHMES cell culture

LUHMES cells [5] were cultured at 37 °C with 5% CO₂ and 100% humidity, as previously described [8, 9]. Briefly, for proliferation, LUHMES cells were cultured in growth medium (GM) consisting of DMEM/F12 (Sigma-Aldrich, St. Louis, MO), 1% N2 supplement (Life Technologies, Carlsbad, CA) and 0.04 µg/mL basic fibroblast growth factor (PeproTech, Rocky Hill, CT) in cell culture flasks (Nunc, Thermo Fisher Scientific, Waltham, MA). Before cell seeding, the flask was pre-coated with poly-L-ornithine (PLO) (0.1 mg/mL, incubation overnight at 37 °C) and washed three times with phosphate buffered saline (PBS; Life Technologies). For differentiation, the cells were seeded in differentiation medium (DM) consisting of DMEM/F12, 1% N2 supplement, 1 µg/mL tetracycline (Sigma-Aldrich), 0.49 µg/mL dibutyl cyclic adenosine monophosphate (Sigma-Aldrich), and 2 ng/mL glial cell-derived neurotrophic factor (R&D Systems, Minneapolis, MN). The experiments were conducted on flasks or multi-well plates (Nunc; ThermoFisher Scientific) double-coated with PLO as described above followed by a second coating with 5 µg/mL fibronectin (R&D Systems) through incubation overnight at 37 °C and washed once with PBS.

Primary neuron preparation

Male mouse pups from the transgenic Thy1- α Syn (Line 61) mouse model [13, 14] were sacrificed on postnatal days D1–3 by decapitation and brains were extracted. The brains were then dissected into small pieces in 4 °C isolation medium containing HibernateTM-A medium (Thermo Fisher Scientific), 1% B-27TM Plus Supplement (Thermo Fisher Scientific), and 0.5 mmol/L L-Glutamine (Sigma Aldrich, G3126). After 2 washes with cold isolation medium, warm Papain (Merck Millipore, Burlington, MA, P4762) Solution (2 mg/mL in HEPES buffer) was added and incubated for 24 min at 37 °C with 5% CO₂, stirred gently every 5 min. To stop the digestion, warm isolation medium was added and the brains were centrifuged at 300 ×g (Heraeus Multifuge 1S-R; ThermoFisher Scientific; acceleration set to 7 and deceleration set to 5) for 10 min at room temperature (RT). After stepwise homogenization in warm isolation medium, the tissue was passed through a 100-µm strainer and centrifuged at 300 ×g (acceleration and deceleration as described above) for 10 min at RT. The pelleted cells were resuspended in cultivation medium containing Neurobasal-A medium (Thermo Fisher Scientific), 1% B-27TM Plus

Supplement, 0.5 mmol/L *L*-Glutamine, and 1% Penicillin/Streptomycin (Thermo Fisher Scientific) and counted.

Primary cell culture

Primary mouse neurons were cultivated in Neurobasal medium (Thermo Fisher Scientific) supplemented with B-27 (50 ×; 2%; Thermo Fisher Scientific), *L*-Glutamine (0.5 nmol/L; Sigma Aldrich) and Penicillin/Streptomycin (100 ×; 1%; Thermo Fisher) on cell culture dishes or multiwell microelectrode array (MEA) plates coated with Poly-*D*-Lysine (50 µg/ml; Sigma Aldrich) at 37 °C with 5% CO₂. Cells were cultivated for 21 days with medium change twice a week until maximum synchrony was reached.

Adenoviral transduction

Adenoviral vectors of serotype 5 (BioFocus, Charles River Laboratories Nederland B.V., Leiden, Netherlands) were used to overexpress human wild-type αSyn or green fluorescent protein (GFP) under a cytomegalovirus promotor. The vectors were not produced within this project but provided by the manufacturer. Briefly, the backbone of the vectors was human mastadenovirus serotype 5 (reference sequence: M73260). In these vectors, nucleotides that contain the E1 region had been deleted and replaced by a polymerase 2 expressing cassette comprising: CMV enhancer/promotor derived from human cytomegaloviruses IE1 gene promotor region, a synthetic region containing polylinker sequences with cDNA sequences inserted into this polylinker, and a SV40 poly(A) signal derived from SV40. Furthermore, the vectors contained an E2 A deletion, in which the E2 A coding region was replaced by a synthetic oligonucleotide. These modifications were performed by the manufacturer to disable the vectors from amplification outside of packaging cells used in the manufacturing process. The αSyn-expressing vectors were provided as 25 µL master aliquots with a titer of 1.7×10^{10} vectors per milliliter. These were diluted in PBS (total 500 µL or 20-fold dilution) to achieve a concentration of 8.5×10^8 vectors per milliliter. The GFP-expressing vectors were provided as 10 µL master aliquot with 5.7×10^{10} vectors per milliliter. These were further diluted in PBS (total 670 µL or 67-fold dilution) to achieve the same concentration of 8.5×10^8 vectors per milliliter. Prior to the transduction, these virus dilutions were further diluted in the cell culture medium to achieve the required multiplicity of infection (MOI). In the high-content screening, in which the cells were seeded in GM, a MOI of 5 (5 viral vectors per seeded cell, 2.5-fold higher than used for transduction of cells seeded in DM; see below) was used to account for proliferation of the cells on the day after seeding. Twenty-four hours after transduction, the remaining

viral vectors were removed by three washes with PBS. In the experiments investigating pathophysiology, the cells were transduced with the vectors two days after seeding in DM with a MOI of 2 (2 viral vectors per seeded cell). The use of lower MOI was because cells that were seeded in DM do not proliferate anymore.

Genome-wide RNA interference screening

In the high-throughput screening, the cells were prepared as in a previous compound screening study [9]. Briefly, cells were seeded in double-coated flasks in GM with medium changed to DM after 24 h. One day after initiation of differentiation, the cells were transduced with adenoviral vectors to overexpress human αSyn. One day later, the remaining virus particles were removed by rinsing the cells with PBS and then the cells were detached using trypsin–EDTA (5 min incubation at 37 °C; Sigma-Aldrich) and reseeded in double-coated 384-well multiwell plates one day after transduction. By doing so, we achieved maximal homogeneity throughout the screening plates. After seeding in the multi-well plates, the cells were treated with different endoribonuclease-prepared small interfering RNAs (esiRNAs). esiRNAs are an RNA interference (RNAi) system with high efficiency and small off-target effects [15, 16]. Cell death was quantified as the percentage of cells with propidium iodide (PI) incorporation. Cell survival was quantified as cells without PI incorporation. PI is an intercalating compound that is actively removed from living cells and therefore accumulates only in dead cells. For the quantification, the cells were incubated with 4 µg/mL PI (Sigma-Aldrich) and 2 µg/mL Hoechst 33342 to stain all cell nuclei. Imaging was performed after 15 min with an Opera High Content Screening System (Perkin Elmer, Waltham, MA).

In the whole screening, a genome-wide library containing esiRNAs against 16,744 genes was tested. Cells transfected with an esiRNA against αSyn were used as a positive control (best survival). Cells transfected with an esiRNA against firefly luciferase (F-Luc), and mock transfected cells, were used as negative control. In the primary screening, the survival of the cells after transfection with all individual esiRNAs was compared to the average survival of the whole library and Z-scores were calculated (Z-statistics). Primary hits were defined as esiRNAs that led to a survival Z-score >2.4 in at least two screening runs compared to the whole library. In total, 46,627 individual experiments were performed.

In the secondary screening, the cells were seeded, transduced with adenoviral vectors, transfected with the esiRNA, and imaged in the same way. In this screening, three runs were performed and an ANOVA followed by a Dunnett's *post-hoc* test was used to compare the survival rate. All esiRNAs that led to a significantly better survival

than the F-Luc esiRNA (P -value <0.05) were considered as secondary hits.

In the tertiary screening, the survival of the cells transfected with these esiRNAs was investigated again in GFP-expressing cells and the survival was compared to the survival of α Syn-overexpressing cells. Those esiRNAs that specifically protected against α Syn as determined by multiple T-tests were considered as final hits.

siRNA transfection

The cells were transfected with either MISSION® esiRNA (Sigma-Aldrich) at a concentration of 200 nmol/L or siPOOL siRNA (SiTOOLS Biotech, Munich, Germany) at a concentration of 5 nmol/L. In preliminary experiments, siPOOL siRNAs were also used at 10 nmol/L. However, we did not observe a higher knockdown efficacy (Supplementary file 1: Fig. S1) and therefore, 5 nmol/L was used for all further experiments. The concentrations were chosen based on the recommendations by the manufacturers. Before distribution, the integrity and purity of individual siPOOLS were verified by high-performance liquid chromatography by the manufacturer. Before transfection, the siRNAs were mixed with OptiMEM medium (Thermo) and Lipofectamine RNAiMax (2 μ L/mL; Thermo Fisher Scientific) and incubated at RT for 20 min. The sequences of used siPOOL siRNAs are shown in Supplementary file 2.

Quantitative real-time polymerase chain reactions (qPCR)

For qPCR, RNA was extracted using the RNeasy Mini kit (Qiagen, Venlo, Netherlands) and RNA concentration was determined with a NanoDrop 2000 (Thermo Fisher Scientific) spectrometer. Subsequently, the RNA samples were reverse transcribed into cDNA using the iScript cDNA Synthesis kit (Bio-Rad Laboratories, Hercules, CA). qPCR was performed with a CFX96 Touch Real-Time PCR Detection System (Bio-Rad Laboratories), using SYBR Select (Thermo Fisher) as dye with the following cycling conditions: an initial denaturation at 95 °C for 10 min, followed by 40 cycles of 95 °C for 15 s and 60 °C for 1 min. The following primers were used for LUHMES cells: *SNX1* forward: AAGCACTCTCAG AATGGCTTC, reverse: CGGCCCTCCGTTTTCAAG; *SNX2* forward: GGGAAGCCCACCGACTTTG, reverse: GGCCATTGGAGTTTGCACTAATA; *SNX5* forward: TCTGTATCTGTGGACCTGAATGT, reverse: GTG GGCAGTGTGGTCTTTGT; *SNX6* forward: TCTTTG AGCAGAACGAACA, reverse: CATCAGCAGCAC TTTTGTGAG; *VPS35* forward: GTCAAGTCATTT CCTCAGTCCAG, reverse: CCCCTCAAGGGATGT TGCAC. The following primers were used for primary

neurons: *SNX5* forward: AGGACCGCAGCAAGTTAA GA; reverse: TGTGGACAGTGTGGTCTTGG.

Western blot

For Western blot, whole cell extracts were collected using M-PER lysis buffer (Thermo Fisher Scientific) supplemented with a protease inhibitor and phosphatase inhibitor cocktail (Merck Millipore) on ice. After centrifugation (15,000 $\times g$ for 10 min at 4 °C), the supernatant was collected and protein content was measured using the BCA Protein assay (Thermo Fisher Scientific) according to the manufacturer's instructions. Proteins (20 μ g) in Laemmli Sample Buffer (Bio-Rad Laboratories) were loaded on 4%–12% bis-tris gels (Bio-Rad Laboratories) or 4%–15% Tris-glycine gels (Bio-Rad). After SDS-PAGE, the proteins were blotted onto methanol-activated polyvinylidene difluoride (PVDF) membranes (0.2 μ m) with a Trans-Blot SD Semi-Dry Transfer Cell system (Bio-Rad Laboratories). After blotting, the membranes were fixed in 0.4% paraformaldehyde (PFA) for 30 min. After rinsing with tris-buffered saline with 0.05% Tween-20 (TBS-T, pH 7.4), the membranes were blocked with 3 \times Rotiblock for 1 h at RT. Thereafter, the membranes were incubated with the primary antibodies in 1 \times Rotiblock in TBS-T overnight at 4 °C, rinsed three times with TBS-T, followed by incubation with a corresponding horse radish peroxidase (HRP)-conjugated secondary antibody in 1 \times Rotiblock in TBS-T for 2 h at RT. After rinsing three times with TBS-T, the membranes were incubated with Clarity ECL substrate (Bio-Rad) for 10–15 min at RT. Images were taken with a LI-COR Odyssey® Fc imaging system (LI-COR Biotechnology, Lincoln, NE). β -Actin or glyceraldehyde 3-phosphate dehydrogenase (GAPDH) served as a loading control.

The following primary antibodies were used: mouse anti-SNX1 (1:1000; Santa Cruz Biotechnology; Dallas, TX), mouse anti-SNX2 (1:1000; Santa Cruz Biotechnology), mouse anti-SNX5 (1:1000; Santa Cruz Biotechnology), mouse anti-SNX6 (1:1000; Santa Cruz Biotechnology), goat anti-VPS35 (1:1000; Abcam, Cambridge, UK), rabbit anti- β -actin (Cell Signaling Technology), and rabbit anti-GAPDH (1:2000; Cell Signaling Technology). The following secondary antibodies were used: HRP-coupled anti-goat, -mouse, or -rabbit antibody (1:5000; Vector Laboratories, Burlingame, CA). A list of all antibodies used in the Western blot analysis is presented in Supplementary file 1: Table S1.

Immunocytochemistry

Sterile glass coverslips (Bellco Glass, Vineland, NJ) in 24-well plates (Nunc) or ibidi dishes (ibidi, Gräfelfing, Germany) were double-coated as described above. For immunocytochemistry, the cells were fixed in 4% PFA

for 30 min at RT followed by permeabilization in Triton X-100 (0.1%; Sigma-Aldrich) for 15 min at RT or Tween-20 (0.1%) for 5 min at RT. After permeabilization, the cells were washed three times with PBS and then blocked with normal horse serum (NHS; 5%; Vector Laboratories) for 1 h at RT or overnight at 4 °C. Thereafter, the cells were incubated with the primary antibodies in NHS (5%) overnight at 4 °C, washed three times with PBS followed by incubation with the secondary antibodies for 2 h at RT. Ten minutes before the end of the incubation period, DAPI (4',6-diamidino-2-phenylindole) (1 µg/mL final concentration) was added to the cells. After three washes with PBS, images were obtained. The following primary antibodies were used: anti-tubulin III (1:000; Santa Cruz Biotechnology), rabbit anti-TGN46 (1:1000; Abcam), mouse anti-Rab5a (1:100; Santa Cruz Biotechnology), rabbit anti-Rab7 (1:100; Abcam), rabbit anti-LAMP1 (1:1000; Abcam), rabbit anti-LAMP2a (1:200; Abcam), rabbit anti-p62 (1:50; Abcam), rabbit anti-LC3B (1:400; Abcam), and rabbit anti-Rab11a (1:1000; Invitrogen). The following secondary antibodies were used: Alexa Fluor 488 donkey anti-mouse or anti-rabbit antibody (1:1000; Thermo Fisher Scientific), Alexa Fluor 594 donkey anti-mouse or anti-rabbit antibody (1:1000; Thermo Fisher Scientific). A list of all antibodies used for immunocytochemistry is presented in Additional file 1: Table S2.

Staining of activated caspases 3/7 (CellEvent™ staining)

On day 8 in vitro (DIV8), the cell culture medium was discarded and cells were incubated with 1 µmol/L CellEvent™ (Thermo Fisher Scientific, 1:1000 dilution) in pre-warmed Hanks'Balanced Salt Solution (HBSS) for 30 min at 37 °C and 5% CO₂. CellEvent™ is a dye that specifically stains activated caspases 3/7 and is therefore used as a marker for apoptosis. After incubation, the solution was replaced with pre-warmed HBSS containing 2 µg/mL Hoechst 33342 (Thermo Fisher Scientific).

Lactate dehydrogenase (LDH) release measurement

Six days after transduction, the cell culture medium was collected to quantify LDH that was released into the cell culture medium as a measure for cytotoxicity. Briefly, 30 µL of conditioned medium was mixed with a reaction buffer containing 74.24 mmol/L Tris/HCl, 185.6 mmol/L NaCl, 3.2 mmol/L pyruvate, and 4 mmol/L nicotinamide adenine dinucleotide (NADH) in water. To measure LDH release, NADH turnover was quantified by repeated measurements of the absorbance at 340 nm over 4 min with a FLUOstar Omega (BMG Labtech, Ortenberg, Germany).

Bafilomycin assay

Bafilomycin A1 (Thermo Fisher, 18029722) was diluted in DMSO to a 100 µmol/L stock solution. Three days after siRNA transfection, primary neurons were treated with 50 µmol/L bafilomycin A1 dissolved in NBBGP – Cultivation medium. Control treatment was established with an equivalent amount of DMSO in the culture medium. The cells were incubated for 24 h. Within this timeframe the cells remained at 37 °C and 5% CO₂.

Multielectrode assay

Primary neurons were plated at a density of 8×10^5 per well directly on top of the electrodes of a CytoView MEA 24 (Axion Biosystems, Atlanta, GA) plate. The plates were pre-coated with 50 µg/mL Poly-D-Lysine several days prior to seeding. The plates were transferred daily into the Maestro Edge MEA system (Axion Biosystems) for evaluation of cellular functions during maturation. After bafilomycin A1 application, the cells remained in the MEA for 24 h with hourly measurements at 37 °C with 5% CO₂. Baseline measurements were performed directly before Bafilomycin A1 application. Data were initially analyzed with the AxIS Navigator (Axion Biosystems).

Treatment with labeled αSyn

Recombinant monomeric αSyn (18 mg/mL) was incubated with ATTO-565-N-hydroxysuccinimidyl-ester (ATTO-TEC, Siegen, Germany) in a sodium bicarbonate buffer according to the manufacturer's instructions to fluorescently label αSyn. After the incubation, the concentration of the resultant solution containing labelled αSyn was adjusted to 2 mg/mL and excess unbound dye was removed using Bio-Spin 6 size exclusion spin columns (Bio-Rad Laboratories). ATT565-αSyn was added to the LUHMES cells on DIV6 at a final concentration of 2 µmol/L. After 24 h, αSyn was removed by three washes with PBS. To remove labeled αSyn on the outside of the cells, the cells were incubated with trypsin–EDTA for 30 s at 37 °C followed by three washes with PBS.

Microscopy and image analysis

All microscopy imaging was performed with a Leica DMI8 inverted fluorescence microscope (Leica Camera AG, Wetzlar, Germany) and Leica Application Suite (LAS) X software. The density of the neuronal network was determined in images stained with the anti-tubulin III antibody by measuring the total branch length as a measure for network density and the number of quadruple points as a measure for network complexity, using a modified version of the 'neurite analyzer' plugin [17] in Fiji (Fiji Is Just ImageJ) version 2.14.0 for Windows 64-bit

(<https://imagej.net/software/fiji/>). An automatized quantification of the CellEvent™ signal intensity in the nuclei region was performed using Fiji.

To quantify the amount of α Syn inside and outside the TGN, a line was drawn across the TGN or Golgi region in each image using LAS X, and the software automatically generated an intensity profile. In each cell analyzed, four regions of interest (ROIs) lines were selected to acquire intensity profiles from both the TGN and adjacent areas. Quantitative analysis was conducted by measuring the area under the curve of the signal intensities inside and outside the TGN region using Fiji. A minimum of 50 cells were evaluated for each experimental condition.

To analyze the colocalization, ROIs were selected by drawing a line across the TGN or Golgi region and the degree of colocalization between α Syn and TGN was quantified using the Fiji software version 2.14.0 for Windows 64-bit with the JACoP plugin, which calculated the thresholded Mander' overlap coefficient (M1t), with thresholds set automatically by the plugin [18].

The different states of the TGN (normal, scattered, and fragmented) were microscopically determined as previously described [19]. A normal TGN has an intact ring shape. A scattered TGN shows a less intensely stained ring shape with some fragments separated from the ring. A fragmented TGN does not show a ring shape, but fragments visible in the cytoplasm.

Statistical analysis

Statistical analysis was performed using GraphPad Prism 10.0 (GraphPad Software, La Jolla, CA). All datasets were tested for normality using the D'Agostino and Pearson omnibus normality test. Unless otherwise specified, one-way ANOVA analysis of variance was performed, followed by a Tukey's *post-hoc* test or pairwise comparisons between selected groups. $P < 0.05$ was considered as statistically significant.

Results

Genome-wide esiRNA screening identified *SNX5* knockdown as being protective against α Syn-induced toxicity

In postmitotic dopaminergic LUHMES neurons that degenerate upon moderate overexpression of human wild-type α Syn [6, 8, 9], we performed a genome-wide esiRNA screening with step-wise validation. In the primary screening, esiRNAs against 16,774 genes were tested for their protective efficacy against α Syn-induced toxicity in duplicates or triplicates, leading to 46,627 experiments in total. Primary hits were selected by a Z-statistic threshold. A secondary screening was conducted to confirm the protectiveness of the hits from the primary screening in comparison to a non-specific control siRNA. A third screening identified those esiRNAs that significantly protected against α Syn-induced toxicity compared to GFP-expressing cells to exclude non-specific effects on cell viability. A flowchart of the screening process is illustrated in Fig. 1a.

Positive hits were defined as esiRNAs leading to a better survival of α Syn-overexpressing cells with a z-Score > 2.4 above the mean survival. In the entire screening, in 1580 wells an esiRNA against α Syn was tested (positive control). Of these, 1246 led to a survival with a Z-score > 2.4 (true positive rate: 79%) and 334 did not meet hit criteria (false-negative rate: 21%). The average Z-score of survival of cells transfected with the esiRNA against α Syn was 3.3 ± 1.8 (standard deviation; SD). An esiRNA against firefly luciferase (F-Luc) was used as negative control. In total, 3964 wells were transfected with the F-Luc esiRNA, 3566 of which yielded a Z-score < 2.4 (true negative rate: 90%), whereas 398 showed a Z-score > 2.4 (false positive rate: 10%). The average Z-score of cells transfected with a F-Luc esiRNA was 1.2 ± 1.2 , suggesting a minor unspecific and non-significant protective effect of the transfection procedure itself. In 1851 wells, a mock transfection was performed, yielding Z-scores < 2.4 in 1849 wells (true

(See figure on next page.)

Fig. 1 Genome-wide siRNA screening. **a** Flowchart of the screening process. Primary screening: Z-statistics ($Z > 2.4$ vs. library) to identify primary hits, defined as $Z > 2.4$ in at least 2 screening runs. Secondary screening: ANOVA analyses (vs. F-Luc as control esiRNA). Tertiary screening, final hits: multiple T-tests (compared to survival of GFP-overexpressing cells). **b** Z-scores of all experiments from the primary screening. Red dots: Z-scores of cells transfected with esiRNA against α Syn as positive control; green dots: Z-scores of cells transfected with esiRNA against luciferase (F-Luc) as negative control; light blue dots: Z-scores from the library; dark blue dots: Z-score > 2.4 ; grey dots: mock transfection. **c** Representative results from one screening plate. Thicker lines mark areas with controls (L: luciferase, M: mock transfection, α : α Syn transfection). **d** Secondary screening results: relative survival compared to the survival of controls (esiRNA against F-Luc). Green bars: increased survival (without correction for multiple testing); light green bars: hits after correction for multiple testing (Dunnett's *post-hoc* test); red bars: reduced survival; light red bars: significant reduction of survival after correction for multiple testing; grey bars: no significant influence on survival. **e** Comparison of the survival between α Syn-overexpressing cells and GFP-expressing cells. Green bars: higher survival in α Syn-overexpressing cells with gene knockdown; light green bars: significantly higher survival after correction for multiple testing. **f** Volcano plot showing the relative survival of α Syn-overexpressing vs GFP-expressing cells. Lower dotted line: P -value < 0.05 in the individual t-tests; upper dotted line: P -value adjusted for multiple testing. SNX5 showed the smallest P -value of all screened genes

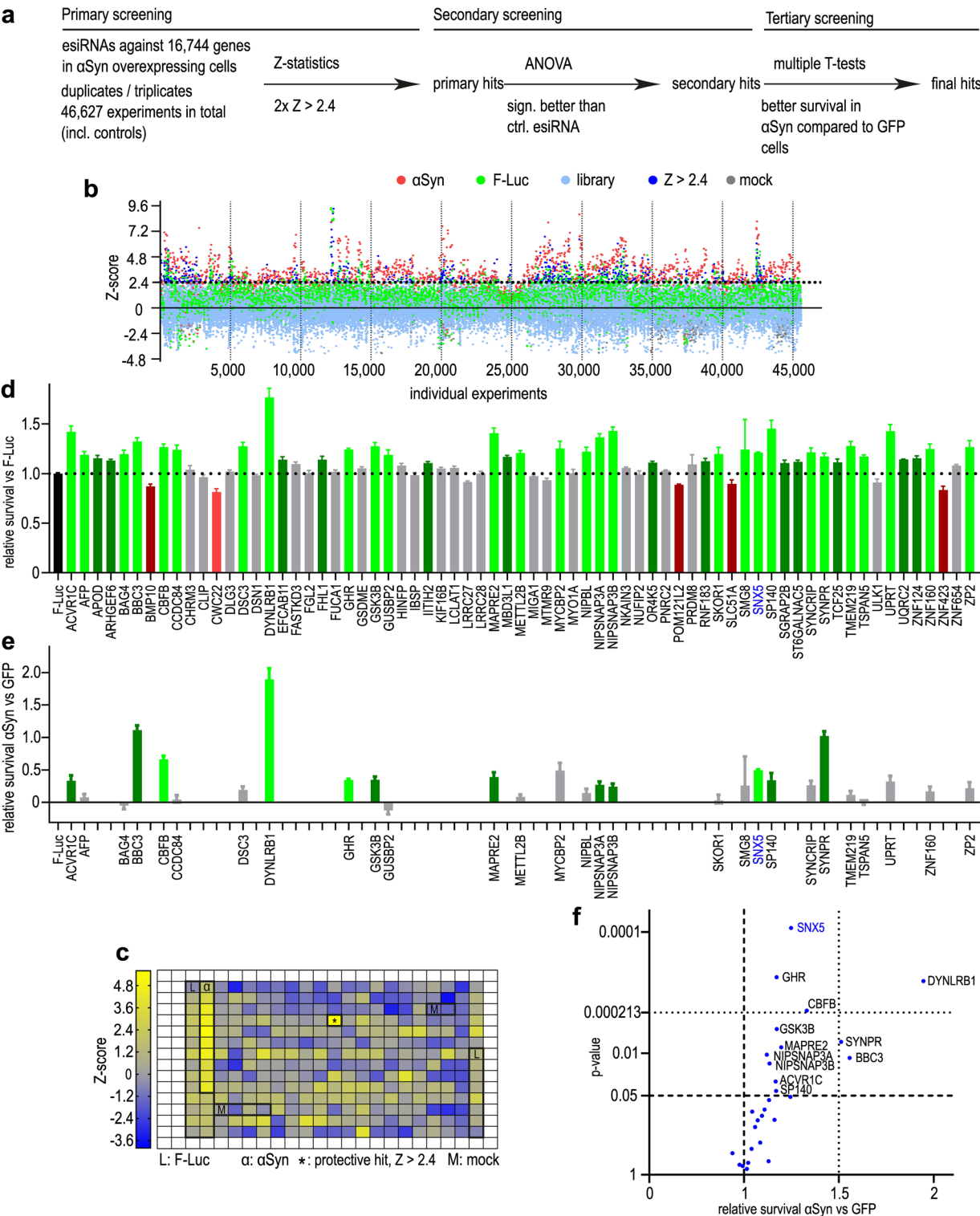


Fig. 1 (See legend on previous page.)

negative rate 100%) with an average Z-score of -0.4 ± 1.0 (SD), showing no effect on cell survival. Results from the complete screening are illustrated in Fig. 1b. The results of an exemplary single plate are displayed in Fig. 1c.

In the primary screening, 80 of the 16,744 esiRNAs led to a higher cell survival in α Syn-overexpressing cells and were therefore selected as primary hits. Eleven of these esiRNAs were excluded because they could not be matched to a protein, were matched to a pseudogene, or were matched to a non-coding RNA. The remaining 69 esiRNAs were tested again in a secondary screening. This secondary screening was performed in order to confirm the protective efficacy of the identified primary hits. To reduce the number of false-positive hits, a more conservative statistical approach was followed in this secondary screening. Cell survival was compared to the survival of cells that had been transfected with a negative-control esiRNA against F-Luc and analyzed using an ANOVA followed by a Dunnett's *post-hoc* test. After correction for multiple testing, 28 esiRNAs led to a significantly higher protection compared to the F-Luc esiRNA control and were therefore considered as confirmed secondary hits (Fig. 1d). In order to exclude unspecific protective effects on cell survival or adenoviral protein overexpression that was independent of α Syn-induced toxicity, we tested these 28 secondary hits again in α Syn-overexpressing cells and in cells that had been transduced with adenoviral vectors to express GFP as control protein. The survival rates of α Syn-overexpressing cells and GFP-expressing cells were compared using multiple *T*-tests. By doing so, we could identify genes whose knockdown specifically protected against α Syn-induced toxicity and had no effect on the general cell viability or on the adenoviral-mediated protein overexpression. Of the 28 secondary hits, 12 protected specifically against α Syn-induced toxicity (*T*-tests), and 4 of them (esiRNAs against *SNX5*, *DYNLRB1*, *CEFB*, and *GHR*) remained significant after correction for multiple testing (Fig. 1e, f). The esiRNA with the lowest *P* value targeted *SNX5*. Therefore, we decided to further elucidate the role of *SNX5* in our PD cell model.

Confirmation of the protective efficacy of *SNX5* knockdown against α Syn-induced toxicity using siPOOL siRNAs

After the screening process, we aimed to confirm the protective efficacy of *SNX5* knockdown against α Syn-induced toxicity with siPOOL siRNAs. LUHMES cells were transduced to overexpress α Syn and transfected with *SNX5*-siRNAs. The knockdown effect and the protective efficacy were determined four and six days after transduction, respectively (Fig. 2a). The siPOOL siRNA efficiently reduced *SNX5* mRNA levels by $93.1\% \pm 42.2\%$

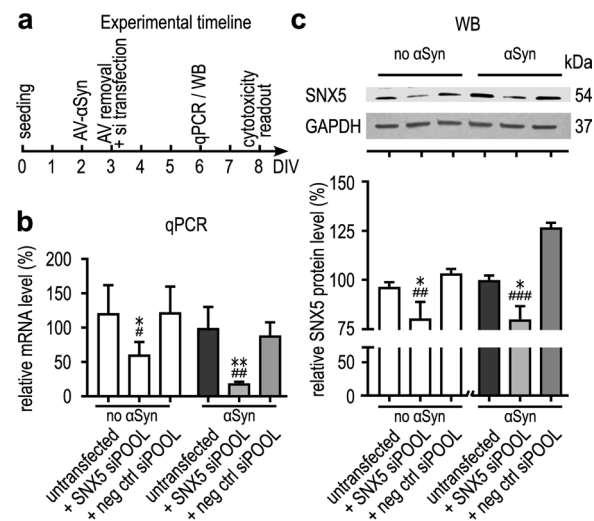


Fig. 2 Validation of the knockdown efficacy of *SNX5* siPOOL siRNAs. **a** Experimental timeline of the validation experiment. AV: adenovirus, DIV: days in vitro. **b** Quantification of *SNX5* mRNA expression in control cells without α Syn overexpression and in α Syn-overexpressing cells by qPCR. Cells were transfected with siPOOL siRNA against *SNX5* or a negative control siRNA, or untransfected. **c** Western blots for *SNX5* and quantitation. The full Western blots are shown in Additional file 3. * $P < 0.05$, ** $P < 0.01$ vs untransfected cells; # $P < 0.05$, ## $P < 0.01$, ### $P < 0.001$ vs cells transfected with a negative control siRNA

($P < 0.001$). The protein level of *SNX5* was also reduced after transfection with siPOOL siRNA against *SNX5*. The *SNX5* protein level in cells treated with a negative control siPOOL siRNA was $126.7\% \pm 1.6\%$ relative to that in the untransfected α Syn-overexpressing cells. After treatment with the siPOOL siRNA against *SNX5*, the *SNX5* protein level was reduced to $80\% \pm 7.1\%$ ($P = 0.03$ vs. untransfected cells, $P < 0.0001$ vs cells transfected with the negative control siPOOL siRNA) (Fig. 2b, c).

Several analyses were performed to determine cell viability. We performed neuronal network analyses (Fig. 3a) and staining of active caspases 3/7 (Fig. 3d). Results of the network analysis showed that the total branch length was 37.2 ± 1.8 mm in untransduced cells, and reduced to 30.2 ± 1.7 mm upon α Syn overexpression ($P < 0.05$). However, knockdown of *SNX5* led to a protection of the neuronal network with total branch lengths of 40.4 ± 0.5 mm ($P < 0.001$ vs untransfected cells and cells transfected with control siRNA; Fig. 3b). In a similar manner, the number of quadruple points as a measure for network complexity was reduced upon α Syn overexpression (77.6 ± 7.7 vs. 107.6 ± 9.2 in untransfected control cells; $P < 0.05$). *SNX5* knockdown preserved the network complexity (121.3 ± 3.2 quadruple points), which was not observed with a negative control siRNA (Fig. 3c). Furthermore, we observed activation of caspases 3/7 upon

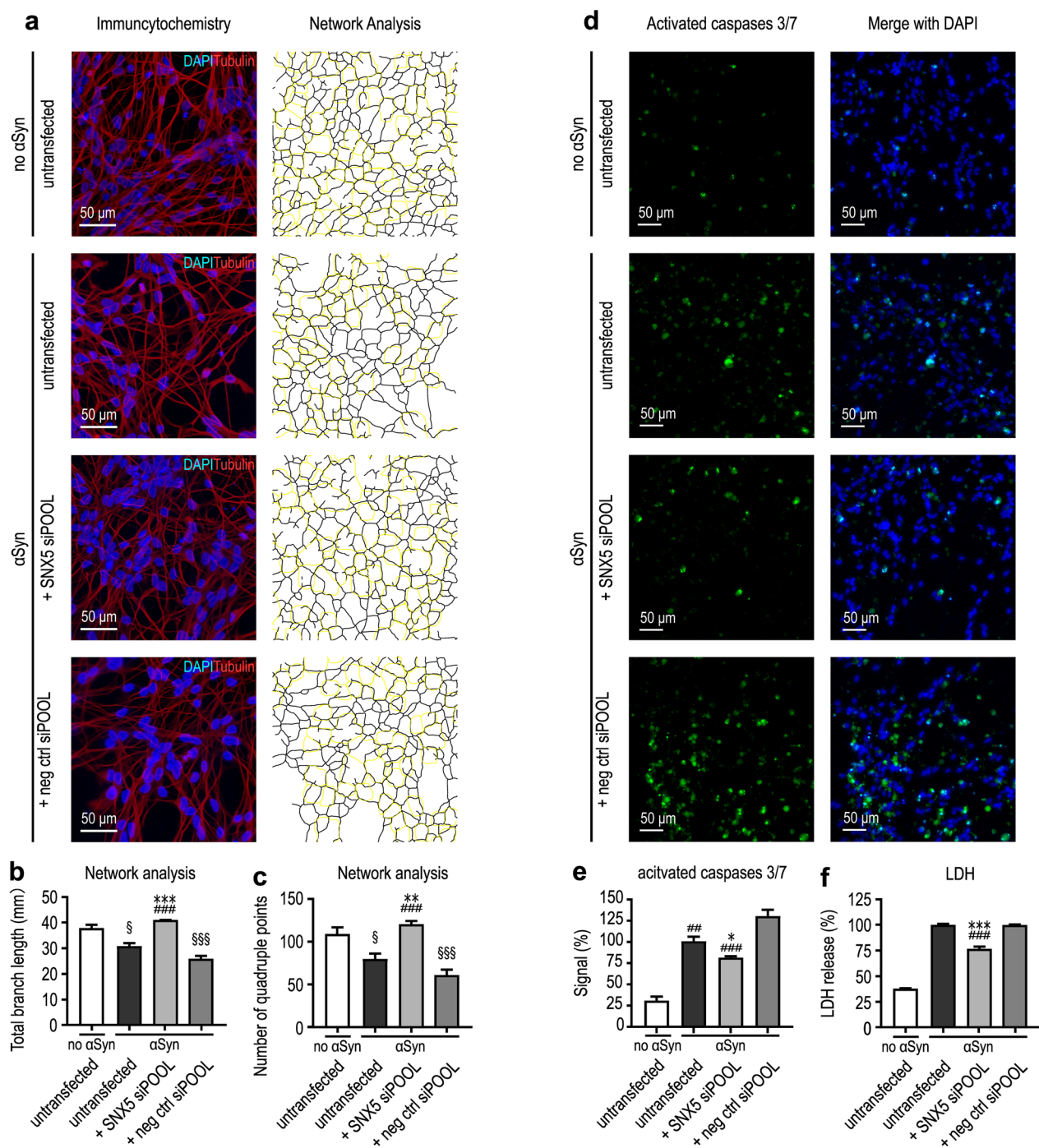


Fig. 3 Validation of the protective efficacy of *SNX5* knockdown against α Syn-induced toxicity. **a** Immunofluorescence images of the neuronal network with an antibody against tubulin III (red) and nuclear co-staining with DAPI (blue) of untransduced cells (no α Syn; top panel), and α Syn-overexpressing cells (α Syn) without and with siRNA transfection. Panels on the right illustrate the neuronal network identified by the 'neurite analyzer' plugin in Fiji. The outline of the nuclei is highlighted in yellow. **b**, **c** Quantification of the total branch length (**b**) and the number of quadruple points as a measure for network complexity (**c**). **d** Immunofluorescence staining for activated caspases 3/7 (green; CellEvent) and nuclear with DAPI (blue). The conditions are the same as in panel **a**. **e** Quantification of the signal of activated caspases 3/7 after normalization to the signal in untransfected AV- α Syn cells. **f** Quantification of LDH released into the cell culture medium as a measure for cytotoxicity at the same conditions as in **a-e**. * $P < 0.05$, ** $P < 0.01$, *** $P < 0.001$, vs untransfected AV- α Syn cells; ## $P < 0.01$, ### $P < 0.001$ vs AV- α Syn cells transfected with a negative control siRNA. § $P < 0.05$, §§§ $P < 0.001$ vs. untransduced cells

α Syn overexpression in LUHMES cells (set to 100%), while in naïve cells, there was only a low signal of activated caspases 3/7 ($30.7\% \pm 4.8\%$). Knockdown of *SNX5* using siPOOL siRNA led to a significant reduction of activated caspases 3/7 to $80.1\% \pm 1.6\%$ ($P = 0.03$), whereas treatment with a negative control siPOOL siRNA led to an increase of activated caspases 3/7 ($129.3\% \pm 7.4\%$) (Fig. 3d, e). Additionally, we quantified LDH release into the cell culture medium as a measure for cell death. In α Syn-overexpressing cells (set to 100%), knockdown of *SNX5* reduced the LDH release by $22.4\% \pm 6.1\%$ ($P < 0.001$), which was not observed after transfection with a negative control siRNA (Fig. 3f). Together, these data confirmed that the knockdown of *SNX5* protected against the α Syn-induced toxicity. The total intracellular or extracellular α Syn levels were not affected by *SNX5* knockdown (Additional file 1: Fig. S2).

Restoration of synchrony loss in primary neurons from α Syn transgenic mice upon *SNX5* knockdown

Primary neurons derived from the Thy1- α Syn PD mouse model [13, 14] were cultivated until they reached maturity (Fig. 4a) indicated by a stable synchronous activity measured in the MEA system. After reaching maturation, the cells were transfected with the siPOOL siRNAs in the same fashion as for the LUHMES cells at 5 nmol/L. Both the siRNA against *SNX5* and the negative control siRNA were well tolerated and did not lead to cell death. Furthermore, we observed effective knockdown. The mRNA expression of *SNX5* was reduced to $6.0\% \pm 0.58\%$ upon transfection with the siPOOL siRNA against *SNX5*, compared to $100\% \pm 8.4\%$ in untransfected cells and

$80.0\% \pm 0.38\%$ in cells transfected with the negative control siRNA (Fig. 4b). This, combined with the high viability, indicated a good tolerability in the primary neurons. Three days post transfection with 5 nmol/L siPOOLS, the cells were exposed to culture medium containing 50 μ mol/L bafilomycin A1 that inhibits autophagy to induce additional stress to these α Syn-overexpressing neurons, reducing their ability to form efficient networks. This was shown by a significant reduction of firing synchrony in response to bafilomycin A1, an observation not made in cells from wild-type mice (data not shown). In untransfected cells the synchrony index was reduced from 0.90 ± 0.01 to 0.73 ± 0.05 ($P = 0.01$) and in cells transfected with the negative control siRNA the synchrony index was reduced from 0.92 ± 0.04 to 0.76 ± 0.05 ($P = 0.02$) upon treatment with bafilomycin A1 (Fig. 4c). In contrast, primary cells with *SNX5* knockdown did not develop a significant reduction of firing synchrony. In cells with *SNX5* knockdown, the synchrony index was 0.92 ± 0.01 without and 0.86 ± 0.03 ($P = 0.55$) with treatment with bafilomycin A1. This indicates a neuroprotective effect of *SNX5* knockdown under these conditions (Fig. 4c).

SNX5 knockdown does not affect the expression of other retromer components

Since *SNX5* protein is a component of the retromer complex (Fig. 5a) as part of the SNX-BAR heterodimers formed by *SNX1/2* and *SNX5/6*, we investigated whether *SNX5* knockdown would lead to changes in the expression of other retromer components, as a possible compensatory mechanism. However, Western blot analysis did not reveal alterations of VPS35 or any of the other

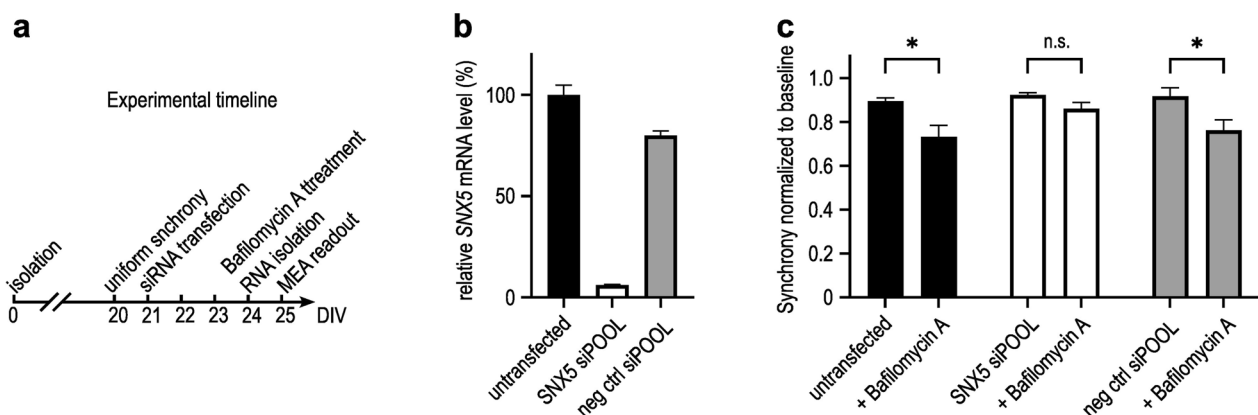


Fig. 4 Restoration of synchrony loss in primary neurons from α Syn transgenic mice upon *SNX5* knockdown. **a** Experimental timeline of primary neuron isolation, maturation and siPOOL application in vitro; DIV, days in vitro. **b** Quantification of *SNX5* mRNA expression in primary neurons from the transgenic Thy1- α Syn (Line 61) mouse model. The cells were transfected with siPOOL siRNAs against *SNX5* or a negative control siRNA, or untransfected. **c** Multiwell microelectrode array (MEA) measurement of neuronal synchrony at 18 h after application of DMSO (left side bars) or 50 μ mol/L bafilomycin A1 in DMSO of the same conditions as described in panel **b**. The graph shows results from 1 out of 3 representative technical replicates; bars represent mean \pm SEM; n.s. = not significant, * $P < 0.05$; Two-way ANOVA with Sidak's post-hoc test

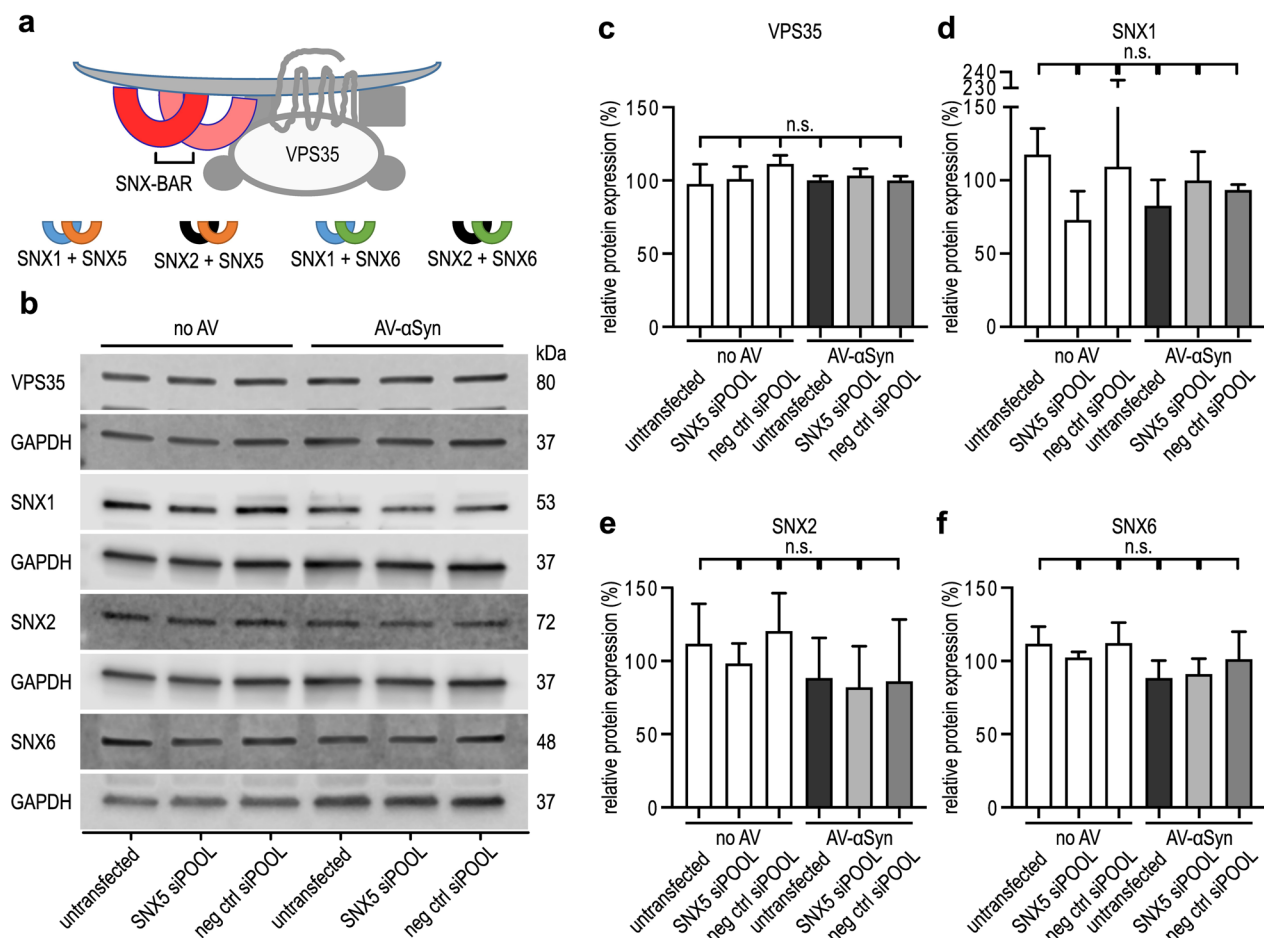


Fig. 5 Effects of SNX5 knockdown on the expression of other retromer components. **a** Schematic illustration of the retromer complex. The SNX-BAR heterodimers are composed of SNX1 (blue arches) or SNX2 (black arches) in combination with SNX5 (orange arches) or SNX6 (green arches). **b** Representative Western blots of other retromer components VPS35, SNX1, SNX2, and SNX6 in AV-αSyn cells and no-αSyn cells. The cells were either untransfected or transfected with siRNA against SNX5 (SNX5 siRNA) or negative control siRNA (neg ctrl). Full Western blots are shown in Additional file 3: Fig. S6 b-e. **c-f** Quantification of the Western blot bands. Neither αSyn overexpression nor SNX5 knockdown (SNX5 siRNA) significantly altered the protein levels of the retromer components VPS35, SNX1, SNX2, and SNX6. Data are shown as mean ± SEM. n.s.: not significant, one-way ANOVA with Tukey's *post-hoc* test

components of the SNX-BAR heterodimers (SNX1, SNX2, SNX6) upon SNX5 knockdown (Fig. 5b–f). However, during investigation of the effects of knockdown of other SNXs, we found that SNX6 knockdown led to a mild increase of LDH release, indicating a toxic effect of SNX6 knockdown (Additional file 1: Fig. S3).

Knockdown of SNX5 prevents the transport of αSyn into the TGN

We next investigated the effect of SNX5 knockdown on the transportation of αSyn within the cells (Fig. 6a). αSyn monomers were fluorescently labelled with ATTO-565 and added to the culture medium.

After fixing the cells, we performed immunocytochemistry staining with a TGN antibody (TGN46) and

analyzed co-localization between αSyn and the TGN area. The TGN area was defined from the fluorescence signal of TGN46 staining (Fig. 6b, c). We then quantified the fluorescence signal of ATTO-αSyn inside and outside this region, and confirmed that extracellularly added αSyn was indeed transported to the TGN region under normal conditions (Fig. 6b, left). Upon SNX5 knockdown, the proportion of ATTO-αSyn inside the TGN region compared to outside the TGN region was shifted towards less αSyn inside the TGN region (Fig. 6b, middle). This effect was not observed upon transfection with a control siRNA (Fig. 6b, right). This suggests that SNX5 knockdown leads to reduced trafficking of αSyn to the TGN.

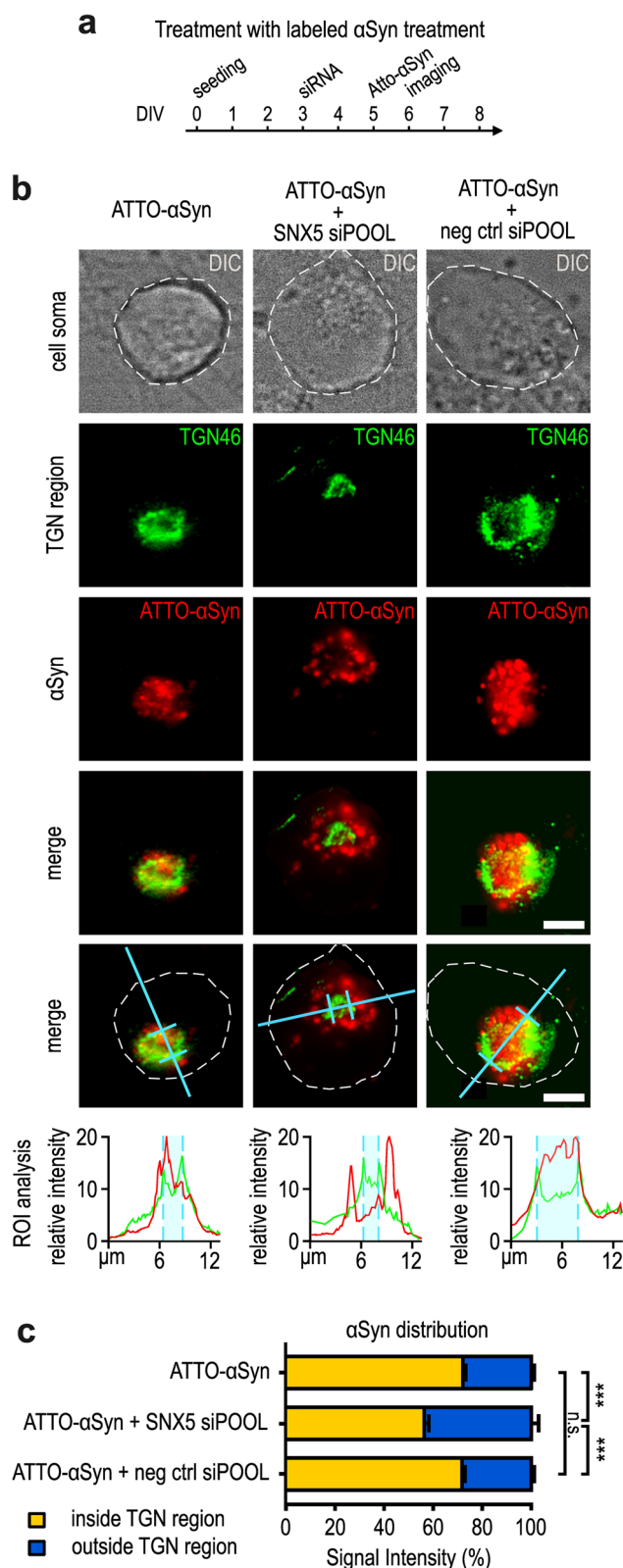


Fig. 6 *SNX5* knockdown prevents internalization and accumulation of exogenous α Syn into the trans-Golgi network. **a** Experimental timeline of the treatment with fluorescently labelled α Syn. DIV, days in vitro. **b** Immunofluorescence staining of TGN46 (green) in cells treated with ATTO-565-labelled α Syn (red). The turquoise lines indicate the location of intensity measurement. Lower panels: The turquoise area in the fluorescence intensity profiles indicate the outer margins of the TGN region, as defined by the TGN46 staining. The red line indicates the location of α Syn, both inside and outside of the TGN. After *SNX5* knockdown, α Syn was distributed outside the TGN as indicated by the red intensity signal (images in the middle), which was not the case with the negative control siRNA (right side images). Scale bar, 4 μ m. **c** Quantification of the proportion of ATTO- α Syn inside and outside of the TGN region in the conditions shown in **b**. *** P < 0.001, ANOVA with Tukey's *post-hoc* test. n.s. not significant

α Syn leads to TGN fragmentation which is ameliorated by *SNX5* knockdown

The morphology of the TGN can be classified into three states: normal, scattered, and fragmented [19]. The different TGN morphologies observed in LUHMES cells exposed to extracellular ATTO- α Syn are shown in Fig. 7a, and their relative quantitative frequency in Fig. 7e. The TGN morphologies in cells transduced to overexpress α Syn (AV- α Syn) are illustrated in Fig. 7b with quantitative data in Fig. 7e.

Then, we studied the effect of *SNX5* knockdown on TGN morphology in the presence of ATTO- α Syn (Fig. 7c) and AV- α Syn (Fig. 7d), using AV-overexpression of GFP as control protein.

Exposure to extracellular ATTO- α Syn or intracellular AV- α Syn overexpression, but not AV-GFP overexpression, led to a significant increase in scattered and fragmented TGN, as compared to untreated control cells. However, this effect was partially prevented by *SNX5*-knockdown, but not by a control siRNA (Fig. 7e).

Furthermore, ATTO- α Syn treatment led to an increase of the TGN diameter from $3.4 \pm 0.1 \mu$ m (untreated controls) to $6.1 \pm 0.2 \mu$ m (P < 0.001). Overexpression of α Syn led to an increase to $6.8 \pm 0.2 \mu$ m (P < 0.001). However, knockdown of *SNX5* prevented this increase, reducing TGN diameter to $3.5 \pm 0.2 \mu$ m in the presence of ATTO- α Syn and $3.6 \pm 0.1 \mu$ m in AV- α Syn transduced cells, with no significant difference compared to untreated or AV-GFP-transduced cells ($3.6 \pm 0.1 \mu$ m; Fig. 7f). To confirm that TGN fragmentation leads to cytotoxicity, we treated the cells with brefeldin A, a compound known to disrupt the TGN [20], and observed increased activity of activated caspases 3/7 as an indicator for cytotoxicity (Additional file 1: Fig. S4).

SNX5 knockdown leads to increased levels of α Syn in early endosomes

To further investigate the mechanism of protection against α Syn-induced toxicity by *SNX5* knockdown, we examined the endosome-to-TGN pathway, the endosome-to-plasma membrane (PM; recycling endosome) pathway, the endosome-to-lysosome pathway, and the autophagosome-to-lysosome pathway.

LUHMES cells were exposed to extracellular ATTO- α Syn either with or without *SNX5* knockdown, prior to fixation for immunocytochemistry. We used an antibody against Rab5a as a marker for early endosomes, antibodies against Rab7 and LAMP1 as markers for late endosomes, an antibody against LAMP2a as a marker for lysosomes, antibodies against p62 and LC3B as markers for autophagosomes, and an antibody against Rab11a as a marker for recycling endosomes (Fig. 8a). Manders' overlap coefficient was determined to evaluate the degree of co-localization between α Syn and the different vesicular structures (Fig. 8b).

Under normal conditions, α Syn showed more co-localization (Manders' overlap coefficient >0.5) with endosomes and lysosomes than with autophagosomes or the recycling endosomes, suggesting that α Syn is mainly transported via the endosome-to-lysosome pathway and accumulates later in lysosomes under normal conditions.

SNX5 knockdown led to a strong increase of co-localization of α Syn with early endosomes (Rab5), from 0.4 ± 0.02 to 0.77 ± 0.02 ($P < 0.001$), and a slight increase of co-localization with late endosome markers Rab7 (from 0.37 ± 0.04 to 0.49 ± 0.02 ; $P < 0.001$) and LAMP1 (from 0.66 ± 0.02 to 0.86 ± 0.02 ; $P < 0.001$). On the other hand, co-localization with autophagosomes and lysosomes was not altered (Fig. 8b). Together with the observation that *SNX5* knockdown led to reduced abundance of α Syn in the TGN (Fig. 6), these observations suggest that *SNX5* facilitates α Syn trafficking from the early endosomes to the TGN (Fig. 9a) and that *SNX5* knockdown reduces this

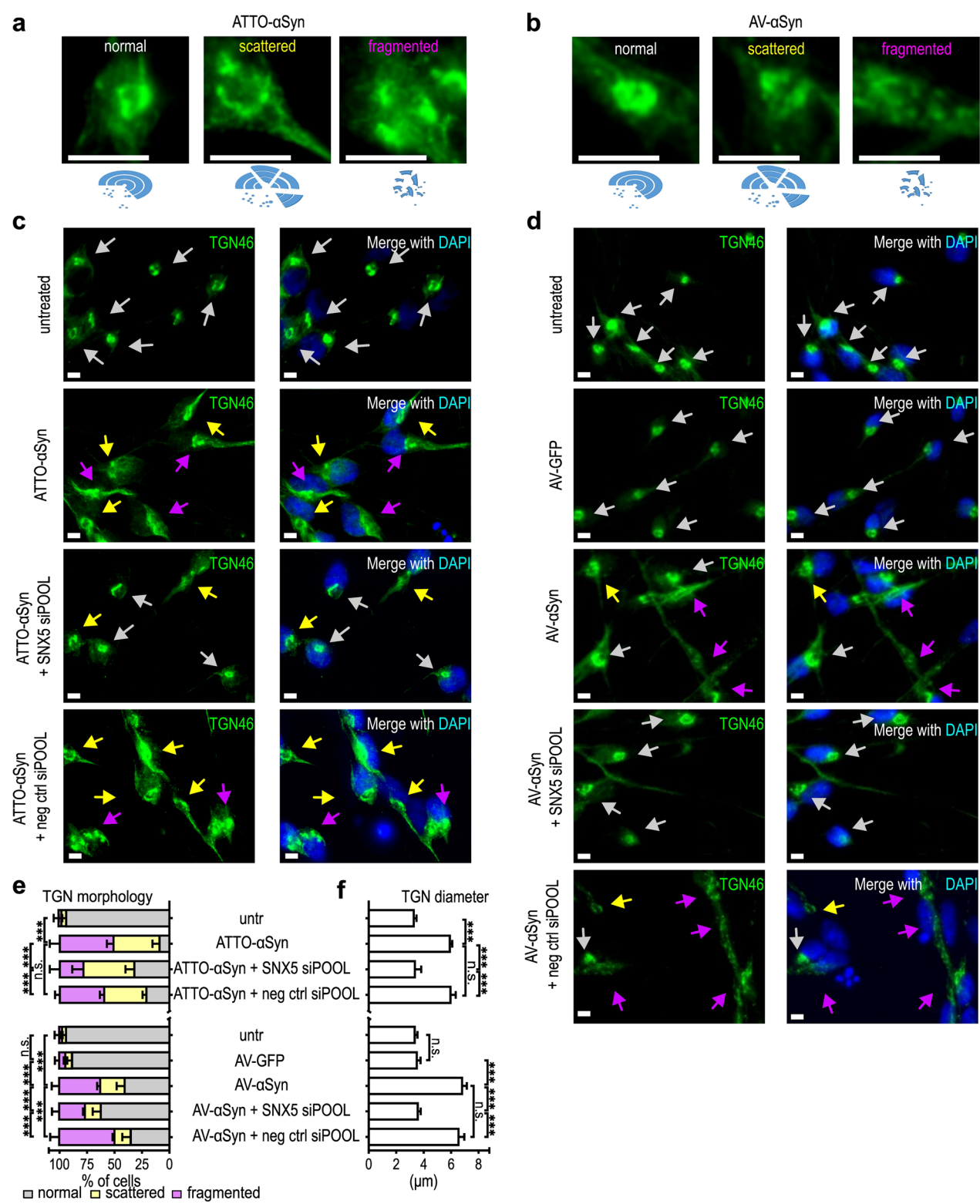
transport and leads to α Syn retention in early and late endosomes (Fig. 9b).

Discussion

In the present work, we conducted a genome-wide multi-step RNAi screening in a PD human neuronal cell model to identify genes whose knockdown can protect against α Syn-induced toxicity. From 69 hits that were identified in the primary screening, 28 were confirmed in the secondary screening. After exclusion of genes whose knockdown unspecifically protected the cells as determined by their effect in GFP-expressing control cells, 12 genes remained, with 4 remaining significant after correction for multiple testing. Amongst these, *SNX5*, a component of the retromer complex, was the most promising candidate to follow-up. We first confirmed the protective efficacy of *SNX5* knockdown with a second RNAi system and by several assays. Furthermore, we used primary neurons derived from transgenic Thy1- α Syn (Line 61) mouse model [13, 14] to confirm the protective efficacy of *SNX5* knockdown. Upon *SNX5* knockdown, we observed a reduced loss of synchrony in these cells. *SNX5* knockdown increased the neuronal network density of α Syn-overexpressing LUHMES cells, reduced activation of caspases 3/7, and decreased LDH release (a measure for reduced cell membrane integrity). Since *SNX5* is part of the SNX-BAR heterodimer within the retromer, we investigated if *SNX5* knockdown led to compensatory regulation of other retromer components, which was not the case. However, we found that in contrast to *SNX5* knockdown, the knockdown of *SNX6*, the alternative for *SNX5* in a possible composition of SNX-BAR heterodimers, increased the α Syn-induced toxicity, suggesting that *SNX5* is involved in the trafficking of toxic α Syn species. We found that α Syn overexpression and treatment with exogenous α Syn led to fragmentation of the TGN, and that *SNX5* knockdown prevented the TGN fragmentation by inhibiting the transport of α Syn to the TGN.

(See figure on next page.)

Fig. 7 *SNX5* knockdown prevents TGN scattering and fragmentation in LUHMES cells. **a** Images of normal, scattered, and fragmented TGN morphology in LUHMES cells treated with ATTO-565-labeled recombinant α Syn monomers. Below are sketches of TGN morphology. All these morphologies were observed in α Syn-treated cells, but at varying degrees. **b** Images of normal, scattered, and fragmented TGN morphology in LUHMES cells transduced with α Syn-overexpressing adenoviral vectors (AV). Below are sketches of TGN morphology. **c** Representative images of staining for TGN46 in untreated cells, ATTO- α Syn-treated cells with no transfection, ATTO- α Syn-treated cells with *SNX5* siRNA transfection, and ATTO- α Syn-treated cells with negative control (neg ctrl) siRNA transfection. The arrows indicate the different states of TGN morphology as illustrated in **a**. White arrows, normal morphology; yellow arrows, scattered morphology; purple arrows, fragmented morphology. A version of this panel that includes red staining of α Syn is shown in Fig. S5. **d** Representative images of staining for TGN46 in control cells (ctrl), AV-GFP cells, AV- α Syn cells, and AV- α Syn cells transfected with *SNX5* siRNA or negative control (neg ctrl) siRNA. **e** Percentage of cells with normal (grey), scattered (yellow), or fragmented (purple) TGN morphology in the experimental conditions of **c** and **d**. Exogenous α Syn (left) as well as adenoviral overexpressed α Syn (right) led to a higher percentage of scattered or fragmented TGNs, which was ameliorated by *SNX5* knockdown. The percentage of abnormal TGN (scattered or fragmented) was subtracted from 100% resulting in values for normal TGN. These were compared using ANOVA with Tukey's *post-hoc* test. **f** Quantification of the TGN diameter of normal and scattered TGN. Both exogenous α Syn (ATTO- α Syn) and adenoviral overexpressed α Syn (AV- α Syn) led to larger TGN sizes. *** $P < 0.001$. ANOVA with Tukey's *post-hoc* test. n.s. not significant



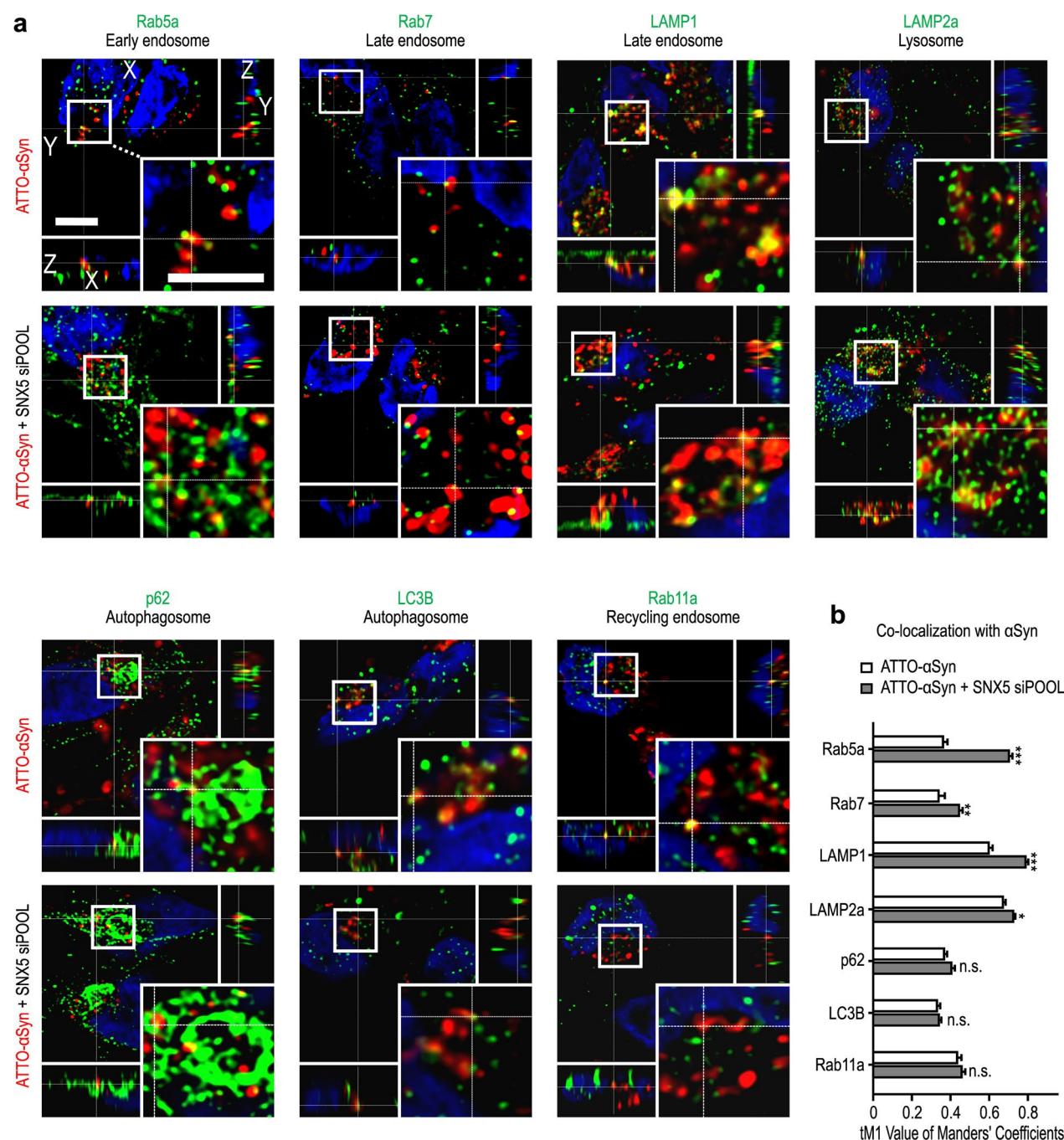


Fig. 8 Co-localization of internalized αSyn with endocytosis markers. **a** Representative images of LUHMES cells treated with fluorescently labeled αSyn (ATTO-αSyn, red) with control siRNA transfection (top row of images), or after knockdown of SNX5 (bottom row of images). A selected region of each image (white square) is shown in higher magnification in the right bottom corner. Scale bars: 4 μm. **b** Quantification of co-localization of exogenous αSyn with endocytosis markers. SNX5 knockdown led to increased co-localization between αSyn and early endosomes (Rab5a), late endosomes (Rab7, LAMP1), and lysosomes (LAMP2a) compared to untransfected cells. Data are presented as mean ± SEM. * $P < 0.05$, ** $P < 0.01$, *** $P < 0.001$ vs ATTO-αSyn, # $P < 0.05$, ## $P < 0.01$, ### $P < 0.001$ vs ATTO-αSyn + SNX5 siRNA; n.s. not significant; one-way ANOVA with Tukey's *post-hoc* test

Our findings suggest that SNX5 is involved in the regulation of the trafficking and toxicity of α Syn and could be a promising target for future development of neuroprotective therapies for PD and related synucleinopathies.

High-throughput RNAi screening is an effective way to identify new genes involved in the pathophysiology of distinct conditions in a hypothesis-free way. However, in the past, RNAi screenings that investigated modifiers of α Syn toxicity were performed only in subsets of the genome and/or in non-human cells (for review see [21]). To our knowledge, we present the first whole-genome RNAi screening of modifiers of α Syn toxicity. Furthermore, we utilized human postmitotic dopaminergic neurons (LUHMES cells), which very closely resemble the dopaminergic cells of the substantia nigra pars compacta, whose demise is responsible for the motor symptoms of PD patients. For the screening, we used a multistep approach to ensure that our final hits specifically modify the α Syn-induced toxicity.

On the one hand, SNX5 was the hit with the lowest *P*-value in the confirmatory screening process. On the other hand, as part of the SNX-BAR heterodimer which itself is part of the retromer, SNX5 is particularly interesting. It is known that the retromer plays a role in the pathophysiology of PD [22–24]. Mutations in VPS35, an important component of the retromer, are risk factors for PD, but the frequency of such mutations is not yet known [25, 26]. Moreover, the retromer is involved in multiple cellular processes including vesicular trafficking, receptor recycling, mitochondrial function and dopamine signaling [25]. In addition, it is currently not yet fully understood if VPS35 mutation leads to a loss or a gain of function of the retromer [26]. Another part of the retromer complex is the SNX-BAR heterodimers (Fig. 3a) composed of SNX1 or SNX2 in combination with SNX5 and SNX6 [27]. The composition of the SNX-BAR heterodimers plays a role in cargo-sorting [28]. Therefore, we hypothesized that SNX5 is involved in the trafficking of toxic α Syn species. This hypothesis was supported by the fact that knockdown of SNX6, the alternative to SNX5 in the SNX-BAR heterodimers, increased toxicity. This observation suggests that the effect of SNX5 knockdown

is specific and not due to the knockdown of retromer components in general.

We then investigated the intracellular localization of exogenously added α Syn in our model and found that upon uptake, α Syn was co-localized with the TGN, suggesting transportation of α Syn to the TGN in our cell model. Other studies have also shown that α Syn co-localizes with the TGN in human astrocytes [29] and in neuroblastoma cells [30]. Furthermore, we observed fragmentation of the TGN as a consequence of α Syn overexpression or treatment with exogenous α Syn. This is consistent with other studies finding that treatment with prefibrillar α Syn aggregates leads to TGN fragmentation in an immortalized fibroblast cell line derived from monkey kidneys [31]. Furthermore, fragmentation of the TGN has been described in nigral neurons of PD patients [32]. Moreover, in other PD cell models, α Syn overexpression leads to Golgi fragmentation [33, 34].

Together, these findings emphasize that our cell model reflects what is observed in patients and supports the relevance of our findings in the present study. Interestingly, SNX5 knockdown prevented trafficking of α Syn to the TGN and its fragmentation, suggesting that SNX5 is a key regulator in the trafficking of toxic α Syn species. A previous study in a yeast model found that α Syn blocks the ER–Golgi transport, and that overexpression of the orthologue of Rab1, a protein needed for the docking of transport vesicles with the Golgi apparatus and thus improving the TGN function, protects dopaminergic neurons from α Syn-induced toxicity in yeast [35]. In line with this study, we could also show that impairment of the TGN is toxic for dopaminergic neurons.

While restoration of the ER–Golgi traffic is one possibility to prevent toxicity, our data suggest that redirection of harmful α Syn species away from the TGN by knocking down SNX5 could also be a strategy to prevent α Syn-induced cell death. Interestingly, we previously showed that α Syn is degraded by macroautophagy and that not only stimulation of autophagy [8] but also bypassing macroautophagy by prevention of the formation of autophagosomes, could protect against α Syn-induced toxicity [7]. These emphasize that in some situations, the stimulation and the bypassing of a specific intracellular

(See figure on next page.)

Fig. 9 Transportation of α Syn before and after knockdown of SNX5. **a, b** Schematic illustration of possible endocytic pathways and the markers of different compartments used in our study (green). After endocytosis from the extracellular space, α Syn is transported into early endosomes (yellow; Rab5a). The early endosomes then either transport α Syn back to the plasma membrane (endosome to PM) in the form of recycling endosomes (Rab11), or to the trans-Golgi network (TGN; TGN46; endosome to TGN), or they form late endosomes (Rab7, LAMP1) to either transport α Syn directly to lysosomes (LAMP2a; endosome to lysosome) or first to autophagosomes (p62, LC3B) and then to lysosomes (autophagosome to lysosome). Before SNX5 knockdown, more α Syn is transported to the TGN, while after SNX5 knockdown less α Syn is transported to the TGN, but more to the early and late endosomes

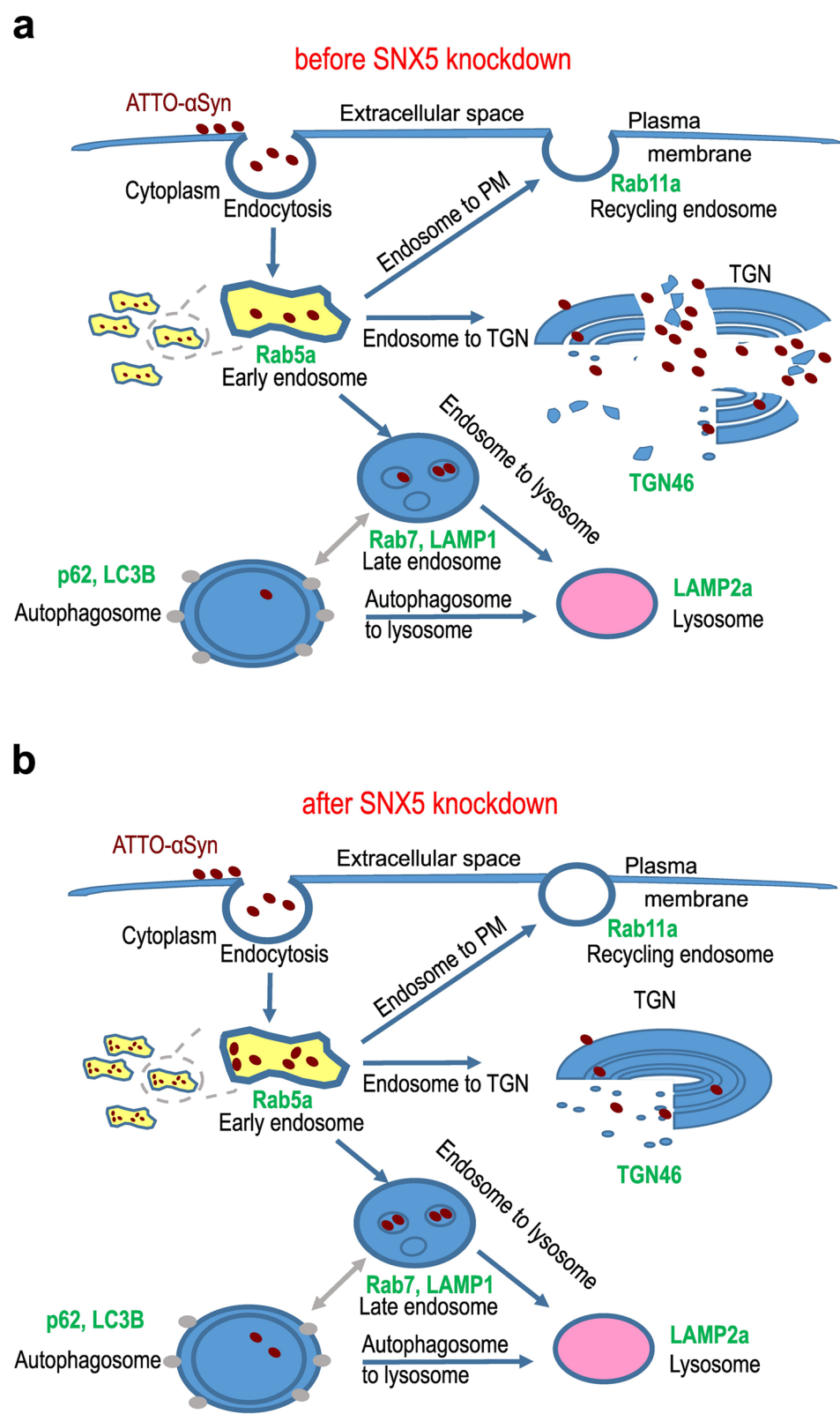


Fig. 9 (See legend on previous page.)

pathway can both be protective. Furthermore, in H4 neuroglial cells, knockdown of distinct Rab GTPases that are involved in α Syn trafficking prevents the formation of α Syn inclusions [36].

However, in other cells, including macrophages, SNX5 is essential for cell functions like micropinocytosis [37]. Furthermore, in mice, SNX5 knockout leads to respiratory failure [38]. Therefore, complete depletion of SNX5 is likely to be detrimental for the whole mechanism. However, reduction of its activity or specific down-regulation in dopaminergic neurons still appears to be a promising approach to reducing the burden of α Syn-induced toxicity in PD.

Conclusion

In summary, we performed a genome-wide siRNA screening and identified SNX5 as the top hit. We found that SNX5 protein as part of the retromer complex is involved in α Syn trafficking. α Syn is taken up and transported to the TGN, leading to TGN fragmentation. Both could be ameliorated by knockdown of SNX5. On the other hand, SNX6 knockdown is toxic to the cells, suggesting that a distinct regulation of intracellular α Syn trafficking involves SNX-BAR heterodimers. Further investigation on α Syn trafficking could lead to the development of new therapeutic options to save neurons from α Syn-induced cell death. In particular, SNX5 seems to be a promising novel target for the development of a neuroprotective treatment for PD and related synucleinopathies.

Abbreviations

α Syn	Alpha-synuclein
BAR	Bin/amphiphysin/Rvs
DAPI	4',6-Diamidino-2-phenylindole
esiRNAs	Endoribonuclease-prepared small interfering RNAs
GFP	Green fluorescent protein
GM	Growth medium
HBSS	Hanks' balanced salt solution
HRP	Horse radish peroxidase
LDH	Lactate dehydrogenase
NADH	Nicotinamide adenine dinucleotide
NHS	Normal horse serum
PD	Parkinson's disease
PFA	Paraformaldehyde
PI	Propidium iodide
RNAi	RNA interference
ROI	Region of interest
SNX5	Sorting nexin 5
TGN	Trans Golgi network
VPS35	Vacuolar protein sorting ortholog 35

Supplementary Information

The online version contains supplementary material available at <https://doi.org/10.1186/s40035-025-00486-5>.

Additional file 1. **Figure S1:** Comparison of different siPOOL concentrations. **Figure S2:** Quantification of α Syn total intracellular and extracellular

levels upon knockdown of SNX5. **Figure S3:** Investigation of the effect of the knockdown of other SNXs. **Figure S4:** Brefeldin A (BFA) treatment led to Golgi fragmentation and cytotoxicity. **Figure S5:** The figure shows a version of panel c of panel 6 from the main manuscript with inclusion of the red channel that shows the signal of labeled α Syn. **Table S1:** Antibodies used for Western blot analysis. **Table S2:** Antibodies used for immunocytochemistry. **Supplementary methods of Brefeldin A treatment.**

Additional file 2. Sequences of used siPOOL siRNAs.

Additional file 3. **Figure S6:** Full Western blots shown in Fig. 2, Fig. 4, and Fig. S2.

Acknowledgements

We thank Sabine Lang (MHH, Dept. for Neurology) for technical support.

Author contributions

MH, LD, OWC, CM, SHB, KL, RK, and KL performed the experiments. FH, FR and CWS reviewed the experimental design. MH, MC, and GUH conceived the study. MH and LD created the figures. MH wrote the first draft of the manuscript. GUH provided overall project leadership. All authors critically revised the manuscript. All authors discussed and commented on the manuscript and agreed to publication.

Funding

Open Access funding enabled and organized by Projekt DEAL. This work was funded by the Deutsche Forschungsgemeinschaft (DFG, German Research Foundation) under Germany's Excellence Strategy within the framework of the Munich Cluster for Systems Neurology (EXC 2145 SyNergy – ID 390857198) and within the Hannover Cluster RESIST (EXC 2155—project number 39087428), the German Federal Ministry of Education and Research (BMBF, 01KU1403 A EpiPD); the ParkinsonFonds Germany (Hypothesis-free compound screen, alpha-Synuclein fragments in PD); Deutsche Forschungsgemeinschaft (DFG, HO2402/18–1 MSAomics); VolkswagenStiftung (Niedersächsisches Vorab); Petermax-Müller Foundation (Etiology and Therapy of Synucleinopathies and Tauopathies), the German Federal Ministry of Education and Research (BMBF, JPND Consortium, SynOD "alpha-Synuclein OMICS to identify Drug-targets" (01ED2405A), Harmonisierung und Re-Analyse vorhandener Datensätze aus einem Zellkulturmodell für Synucleinopathien (01ED2405B)).

Availability of data and materials

All datasets used and analyzed in this study are available from the corresponding authors on reasonable request.

Declarations

Ethics approval and consent to participate

Not applicable.

Consent for publication

Not applicable.

Competing interests

All authors have no competing interests.

Author details

¹Department of Neurology, Hannover Medical School, Carl-Neuberg-Str. 1, 30625 Hannover, Germany. ²Center for Systems Neuroscience, Hannover, Germany. ³HT-Technology Development Studio, Max Planck Institute of Molecular Cell Biology and Genetics, Dresden, Germany. ⁴Department of Pharmacology, Toxicology and Pharmacy, University of Veterinary Medicine Hannover, Hannover, Germany. ⁵Department of Neurology, LMU University Hospital, Ludwig-Maximilians-Universität (LMU), Munich, Germany. ⁶The Institute of Cardiovascular Physiology and Pathophysiology, Ludwig-Maximilians-Universität (LMU), Munich, Germany. ⁷German Center for Neurodegenerative Diseases (DZNE), Munich, Germany. ⁸Munich Cluster for Systems Neurology (SyNergy), Munich, Germany.

Received: 23 April 2024 Accepted: 27 April 2025
Published online: 03 June 2025

References

- Goedert M, Spillantini MG, Del Tredici K, Braak H. 100 years of Lewy pathology. *Nat Rev Neurol*. 2013;9(1):13–24.
- Fanciulli A, Stankovic I, Krismer F, Seppi K, Levin J, Wenning GK. Multiple system atrophy. *Int Rev Neurobiol*. 2019;149:137–92.
- Tofaris GK. Initiation and progression of α -synuclein pathology in Parkinson's disease. *Cell Mol Life Sci*. 2022;79(4):210.
- Burré J, Sharma M, Südhof TC. Cell biology and pathophysiology of α -synuclein. *Cold Spring Harb Perspect Med*. 2018;8(3):a024091.
- Lotharius J, Falsig J, van Beek J, Payne S, Dringen R, Brundin P, et al. Progressive degeneration of human mesencephalic neuron-derived cells triggered by dopamine-dependent oxidative stress is dependent on the mixed-lineage kinase pathway. *J Neurosci*. 2005;25(27):6329–42.
- Höllerhage M, Goebel JN, de Andrade A, Hildebrandt T, Dolga A, Culmsee C, et al. Trifluoperazine rescues human dopaminergic cells from wild-type α -synuclein-induced toxicity. *Neurobiol Aging*. 2014;35(7):1700–11.
- Fussi N, Höllerhage M, Chakraborty T, Nykänen N-P, Rösler TW, Koeglsperger T, et al. Exosomal secretion of α -synuclein as protective mechanism after upstream blockage of macroautophagy. *Cell Death Dis*. 2018;9(7):757.
- Höllerhage M, Fussi N, Rösler TW, Wurst W, Behrends C, Höglinger GU. Multiple molecular pathways stimulating macroautophagy protect from α -synuclein-induced toxicity in human neurons. *Neuropharmacology*. 2019;149:13–26.
- Höllerhage M, Moebius C, Melms J, Chiu W-H, Goebel JN, Chakraborty T, et al. Protective efficacy of phosphodiesterase-1 inhibition against α -synuclein toxicity revealed by compound screening in LUHMES cells. *Sci Rep*. 2017;7(1):11469.
- Harbour ME, Breusegem SYA, Antrobus R, Freeman C, Reid E, Seaman MNJ. The cargo-selective retromer complex is a recruiting hub for protein complexes that regulate endosomal tubule dynamics. *J Cell Sci*. 2010;123(Pt 21):3703–17.
- Harbuz L, Marano MM, Tandon A. Import and export of misfolded α -synuclein. *Front Neurosci*. 2018;12:344.
- Follett J, Norwood SJ, Hamilton NA, Mohan M, Kovtun O, Tay S, et al. The Vps35 D620N mutation linked to Parkinson's disease disrupts the cargo sorting function of retromer. *Traffic*. 2014;15(2):230–44.
- Chesneau M-F, Richter F. Modelling of Parkinson's disease in mice. *Lancet Neurol*. 2011;10(12):1108–18.
- Richter F, Stanojlovic M, Käufer C, Gericke B, Feja M. A mouse model to test novel therapeutics for Parkinson's disease: an update on the Thy1-aSyn ("line 61") mice. *Neurotherapeutics*. 2023;20(1):97–116.
- Kittler R, Surendranath V, Heninger A-K, Slabicki M, Theis M, Putz G, et al. Genome-wide resources of endoribonuclease-prepared short interfering RNAs for specific loss-of-function studies. *Nat Methods*. 2007;4(4):337–44.
- Theis M, Buchholz F. MISSION esiRNA for RNAi screening in mammalian cells. *J Vis Exp*. 2010;39:2008.
- Haas AJ, Prigent S, Dutertre S, Le Dréan Y, Le Page Y. Neurite analyzer: an original Fiji plugin for quantification of neuriteogenesis in two-dimensional images. *J Neurosci Methods*. 2016;271:86–91.
- Hoffmann A-C, Minakaki G, Menges S, Salvi R, Savitskiy S, Kazman A, et al. Extracellular aggregated α -synuclein primarily triggers lysosomal dysfunction in neural cells prevented by trehalose. *Sci Rep*. 2019;9(1):544.
- Paiva I, Jain G, Lázaro DF, Jerčić KG, Hentrich T, Kerimoglu C, et al. α -Synuclein deregulates the expression of COL4A2 and impairs ER-Golgi function. *Neurobiol Dis*. 2018;119:121–35.
- Dinter A, Berger EG. Golgi-disturbing agents. *Histochem Cell Biol*. 1998;109(5–6):571–90.
- Höllerhage M, Bickle M, Höglinger GU. Unbiased screens for modifiers of α -synuclein toxicity. *Curr Neurol Neurosci Rep*. 2019;19(2):8.
- Cui Y, Yang Z, Teasdale RD. The functional roles of retromer in Parkinson's disease. *FEBS Lett*. 2018;592(7):1096–112.
- Yang Z, Li Z, Teasdale RD. Retromer dependent changes in cellular homeostasis and Parkinson's disease. *Essays Biochem*. 2021;65(7):987–98.
- Williams ET, Chen X, Moore DJ. VPS35, the retromer complex and Parkinson's disease. *J Parkinsons Dis*. 2017;7(2):219–33.
- Rahman AA, Morrison BE. Contributions of VPS35 mutations to Parkinson's disease. *Neuroscience*. 2019;401:1–10.
- Sassone J, Reale C, Dati G, Regoni M, Pellicchia MT, Garavaglia B. The role of VPS35 in the pathobiology of Parkinson's disease. *Cell Mol Neurobiol*. 2021;41(2):199–227.
- Simonetti B, Danson CM, Heesom KJ, Cullen PJ. Sequence-dependent cargo recognition by SNX-BARs mediates retromer-independent transport of Cl-MPR. *J Cell Biol*. 2017;216(11):3695–712.
- Kvainickas A, Jimenez-Organ A, Nägela H, Hu Z, Dengjel J, Steinberg F. Cargo-selective SNX-BAR proteins mediate retromer trimer independent retrograde transport. *J Cell Biol*. 2017;216(11):3677–93.
- Rostami J, Holmqvist S, Lindström V, Sigvardson J, Westermark GT, Ingels-Son M, et al. Human astrocytes transfer aggregated α -synuclein via tunneling nanotubes. *J Neurosci*. 2017;37(49):11835–53.
- Hivare P, Gadhavi J, Bhatia D, Gupta S. α -Synuclein fibrils explore actin-mediated macropinocytosis for cellular entry into model neuroblastoma neurons. *Traffic*. 2022;23(7):391–410.
- Gosavi N, Lee H-J, Lee JS, Patel S, Lee S-J. Golgi fragmentation occurs in the cells with prefibrillar α -synuclein aggregates and precedes the formation of fibrillar inclusion. *J Biol Chem*. 2002;277(50):48984–92.
- Fujita Y, Ohama E, Takatama M, Al-Sarraj S, Okamoto K. Fragmentation of Golgi apparatus of nigral neurons with α -synuclein-positive inclusions in patients with Parkinson's disease. *Acta Neuropathol*. 2006;112(3):261–5.
- Martínez-Menárguez JA, Tomás M, Martínez-Martínez N, Martínez-Alonso E. Golgi fragmentation in neurodegenerative diseases: is there a common cause? *Cells*. 2019;8(7):748.
- Nakagami S, Barsom MJ, Bossy-Wetzel E, Sütterlin C, Malhotra V, Lipton SA. A Golgi fragmentation pathway in neurodegeneration. *Neurobiol Dis*. 2008;29(2):221–31.
- Cooper AA, Gitler AD, Cashikar A, Haynes CM, Hill KJ, Bhullar B, et al. α -Synuclein blocks ER-Golgi traffic and Rab1 rescues neuron loss in Parkinson's models. *Science*. 2006;313(5785):324–8.
- Gonçalves SA, Macedo D, Raquel H, Simões PD, Giorgini F, Ramalho JS, et al. shRNA-based screen identifies endocytic recycling pathway components that act as genetic modifiers of α -synuclein aggregation, secretion and toxicity. *PLoS Genet*. 2016;12(4):e1005995.
- Lim JP, Teasdale RD, Gleeson PA. SNX5 is essential for efficient macropinocytosis and antigen processing in primary macrophages. *Biol Open*. 2012;1(9):904–14.
- Im S-K, Jeong H, Jeong H-W, Kim K-T, Hwang D, Ikegami M, et al. Disruption of sorting nexin 5 causes respiratory failure associated with undifferentiated alveolar epithelial type I cells in mice. *PLoS One*. 2013;8(3):e58511.